Electron impact excitation of NIV: Calculations with the DARC code and a comparison with ICFT results

Monthly Notices
of the
ROYAL ASTRONOMICAL SOCIETY

MNRAS **461,** 3997–4012 (2016) doi:10.1093/mnras/stw1369

Electron impact excitation of N IV: calculations with the DARC code and a comparison with ICFT results

K. M. Aggarwal,[1]★ F. P. Keenan[1] and K. D. Lawson[2]

[1]*Astrophysics Research Centre, School of Mathematics and Physics, Queen's University Belfast, Belfast BT7 1NN, UK*
[2]*CCFE, Culham Science Centre, Abingdon OX14 3DB, UK*

Accepted 2016 June 3. Received 2016 June 2; in original form 2016 April 14

ABSTRACT

There have been discussions in the recent literature regarding the accuracy of the available electron impact excitation rates (equivalently effective collision strengths Υ) for transitions in Be-like ions. In the present paper we demonstrate, once again, that earlier results for Υ are indeed overestimated (by up to four orders of magnitude), for over 40 per cent of transitions and over a wide range of temperatures. To do this we have performed two sets of calculations for N IV, with two different model sizes consisting of 166 and 238 fine-structure energy levels. As in our previous work, for the determination of atomic structure the GRASP (General-purpose Relativistic Atomic Structure Package) is adopted and for the scattering calculations (the standard and parallelised versions of) the Dirac Atomic R-matrix Code (DARC) are employed. Calculations for collision strengths and effective collision strengths have been performed over a wide range of energy (up to 45 Ryd) and temperature (up to 2.0×10^6 K), useful for applications in a variety of plasmas. Corresponding results for energy levels, lifetimes and A-values for all E1, E2, M1 and M2 transitions among 238 levels of N IV are also reported.

Key words: atomic data – atomic processes.

1 INTRODUCTION

Emission lines from Be-like ions have provided useful electron density and temperature diagnostics for a variety of astrophysical plasmas. Many ions in this series, such as C III, N IV, Ti XIX and Fe XXIII, are also important for the study of fusion plasmas. For N IV Chaplin et al. (2009) have measured the $2s^2\ {}^1S_0$–$2s2p\ {}^1P^o_1$ line at 76.5 nm in the Swarthmore Spheromak Experiment to diagnose the plasma impurities. Similarly, Machida et al. (2009) have measured three impurity lines of N IV (λ 765, 923 and 1719 Å) in the NOVA-UNICAMP tokamak plasma. However, for plasma modelling accurate atomic data are required, particularly for energy levels, radiative rates (A-values), and excitation rates or equivalently the effective collision strengths (Υ), which are obtained from the electron impact collision strengths (Ω). Given that, we have already reported such data for a number of Be-like ions, namely C III, Al X, Cl XIV, K XVI, Ti XIX and Ge XXIX - see Aggarwal & Keenan (2015a,b) and references therein. In this paper we focus our attention on N IV.

Several emission lines of N IV have been observed in the Sun (Dufton, Doyle & Kingston 1979). In addition, forbidden lines, mostly belonging to the $2s^2\ {}^1S$ – $2s2p\ {}^3P^o$ multiplet (λλ 1483,1486 Å), have been observed in the ultraviolet spectra of low-density astrophysical plasmas, such as planetary nebulae and symbiotic stars – see for example, Feibelman, Aller & Hyung (1992) and Doschek & Feibelman (1993). These doublet lines are also detected in Ly α emitting galaxies (Fosbury et al. 2003 and Vanzella et al. 2010) and in low-mass and low-luminosity galaxies (Stark et al. 2014).

An early analysis of solar emission lines of N IV was undertaken by Dufton et al. (1979). In the absence of direct calculations of collisional data, they interpolated Υ from the existing results for C III and O V. Subsequently, Ramsbottom et al. (1994) calculated such data adopting the R-matrix code. These calculations are in *LS* coupling (Russell–Saunders or spin-orbit coupling) and include the 12 states of the $2s^2$, 2s2p, $2p^2$ and $2s3\ell$ configurations. Subsequent results for fine-structure transitions were obtained through an algebraic re-coupling scheme, and stored in an earlier version of the CHIANTI data base at http://www.chiantidatabase.org/.

Recently, Fernández-Menchero, Del Zanna & Badnell (2014) have performed much larger calculations for a series of Be-like ions, including N IV. They have considered 238 fine-structure levels, belonging to the $n \leq 7$ configurations. For the generation of wave functions, i.e. to determine energy levels and A-values, they adopted the *AutoStructure* (AS) code of Badnell (1997) and for the subsequent calculations of Ω and Υ, the R-matrix code of Berrington, Eissner & Norrington (1995). However, they also primarily obtained Ω in *LS* coupling, and the corresponding results for fine-structure transitions were determined through their intermediate coupling frame transformation (ICFT) method, similar to

★E-mail: K.Aggarwal@qub.ac.uk

the one adopted by Ramsbottom et al. (1994). The AS code does not include higher order relativistic effects, which are important for heavier systems (such as Ge XXIX), but not for a comparatively light ion, such as N IV. Therefore, their calculations should represent a significant extension and improvement over the earlier results of Ramsbottom et al. (1994). However, our work on a number of Be-like ions (Al X, Cl XIV, K XVI, Ti XIX and Ge XXIX) indicated that the data of Fernández-Menchero et al. (2014) were highly overestimated for a significant number of transitions, and over a wide range of electron temperatures (Aggarwal & Keenan 2015a). These Be-like ions are comparatively highly ionized, but similar discrepancies have also been noted for transitions in C III (Aggarwal & Keenan 2015b) as well as for Al-like Fe XIV (Aggarwal & Keenan 2014), and most recently for Ar-like Fe IX (Tayal & Zatsarinny 2015).

No two independent atomic data calculations are ever exactly the same, but there are two major differences between our work and that of Fernández-Menchero et al. (2014), namely the methodology and the size. For the scattering calculations we have adopted the fully relativistic Dirac atomic R-matrix code (DARC), in comparison to their semi-relativistic R-matrix method through the ICFT approach. However, in principle both approaches should provide comparable results for a majority of transitions and over a wide range of temperature, as has already been observed in several cases – see for example the work of Badnell & Ballance (2014) on Fe III and references therein. Therefore, the discrepancies noted in the values of Υ for a range of Be-like ions are perhaps not due to the methodologies but their implementation, as already discussed in detail by us (Aggarwal & Keenan 2015a). Since such large discrepancies are worrying and need to be addressed so that data can be confidently applied to plasma modelling, Fernández-Menchero, Del Zanna & Badnell (2015) made an extensive analysis of these discrepancies taking Al X as an example. They rather concluded that the differences in the calculations of Υ lie in the corresponding differences in the determination of *atomic structure*, and not in the implementation of the scattering methods as we suggested. Since they could perform much larger calculations than us (and indeed others such as Tayal & Zatsarinny 2015), they not only defended their work but also concluded their results to be more accurate. In general, it is undoubtedly true that a larger calculation should be superior (i.e. comparatively more accurate), because of the inclusion of resonances arising from the higher-lying levels of the additional configurations. However, these should not increase values of Υ by orders of magnitude, and not for a significant number of transitions and over an entire range of temperatures. Unfortunately, until now it was not possible for us to match the size of the Fernández-Menchero et al. (2014) calculations, because of the limitations of the computational resources available to us. However, one of our colleagues (Dr Connor Ballance) has now implemented the parallelised version of the DARC code and therefore we are able to perform as large a calculation as Fernández-Menchero et al. (2014, 2015). We do this for an important Be-like ion, i.e. N IV, to make direct comparisons with their work.

2 ENERGY LEVELS

As in our earlier work on other Be-like ions, we have employed the fully relativistic GRASP (General-purpose Relativistic Atomic Structure Package) to determine the atomic structure, i.e. to calculate energy levels and A-values. Measurements of energy levels for N IV have been compiled and critically evaluated by the NIST (National Institute of Standards and Technology) team (Kramida et al. 2015) and are available at their website http://www.nist.gov/pml/data/asd.cfm. However, these energies are restricted to mostly low-lying levels and are missing for many of the $n \geq 4$ configurations – see Table 1. Theoretical energies have been determined by several workers – see for example, Gu (2005) and references therein – but these are also restricted to a few lower levels, mostly up to $n = 3$. However, as stated earlier, Fernández-Menchero et al. (2014) have determined energies for 238 levels belonging to the $n \leq 7$ configurations. In our work, we have performed two sets of calculations, i.e. GRASP1: which includes 166 levels of 27 configurations, namely $(1s^2)\ 2\ell 2\ell'$, $2\ell 3\ell'$, $2\ell 4\ell'$ and $2\ell 5\ell'$. These calculations are similar to those for C III (Aggarwal & Keenan 2015b), but larger than for other Be-like ions we have investigated (Aggarwal & Keenan 2015a), which were confined to the lowest 98 levels. For the other (GRASP2) calculation we include the same 238 levels as by Fernández-Menchero et al. (2014), the additional 72 levels belonging to $(1s^2)$ 2s6s/p/d, 2p6s/p/d, 2s7s/p/d, and 2p7s/p/d, i.e. 39 configurations in total. Both calculations have been performed in an 'extended average level' approximation and include contributions from the Breit and QED (quantum electrodynamic) effects. These energies are listed in Table 1 along with those of NIST and Fernández-Menchero et al. (2014).

The GRASP1 and GRASP2 energies are nearly the same, in both magnitude and ordering. Similarly, there is a general agreement (within 0.02 Ryd or 1 per cent for all levels) between our GRASP and the earlier AS energies of Fernández-Menchero et al. (2014), and the orderings are also nearly the same for most levels with only a few exceptions – see for example, levels 94–95, 98–101 and 149–151. However, differences with the NIST energies are significant (up to 6 per cent), particularly for the lowest 10 levels of the 2s2p and $2p^2$ configurations – see Fig. 1. Fortunately, discrepancies for the remaining levels are smaller than 1 per cent. We also note that level 107 ($2p4p\ ^3S_1$) is an exception, because its placing in the NIST listings is anomalous with results to that from GRASP and AS, and theoretical energies for this level are lower by ∼0.1 Ryd. In the absence of any other calculation it is difficult to resolve its position, and results for C III do not help because the level orderings of the two ions are very different – see table 1 of Aggarwal & Keenan (2015b). However, all four $J = 1$ levels of the 2p4p configuration, i.e. 94 ($^1P_1$), 96 ($^3D_1$), 107 ($^3S_1$) and 109 ($^3P_1$), are highly mixed, and interchanging their positions will not resolve the discrepancy in the energies, as none has a value closer to that of NIST. Additionally, the level mixing is strong only in *jj* coupling and there is no ambiguity in *LSJ* coupling. Finally, we observe better agreement between theoretical and experimental energies for the levels of N IV than for C III (Aggarwal & Keenan 2015b), but scope remains for improvement. An inclusion of *pseudo* orbitals in the generation of wave functions may improve the accuracy of energy levels, but it will give rise to pseudo resonances in the subsequent scattering calculations for Ω. Therefore, both ourselves and Fernández-Menchero et al. (2014) have avoided this approach because the focus is on electron impact excitation.

3 RADIATIVE RATES

Generally, A-values for electric dipole (E1) transitions alone are not sufficient for plasma modelling applications, even though they have larger magnitudes in comparison to other types, namely electric quadrupole (E2), magnetic dipole (M1) and magnetic quadrupole (M2). Hence for completeness and also for the accurate determination of lifetimes (see Section 4) we have calculated A-values for all four types of transitions. Furthermore, although A-values are often directly employed in plasma modelling calculations, it is the

Table 1. Energy levels (in Ryd) of N IV and their lifetimes (s). $a \pm b \equiv a \times 10^{\pm b}$.

Index	Configuration	Level	NIST	GRASP1	GRASP2	AS	GRASP1(τ, s)	GRASP2(τ, s)
1	$2s^2$	$^1S_0$	0.000 00	0.000 00	0.000 00	0.000 00	.....	.....
2	2s2p	$^3P^o_0$	0.612 46	0.618 45	0.617 94	0.623 31	.....	.....
3	2s2p	$^3P^o_1$	0.613 03	0.618 98	0.618 48	0.624 08	2.471−03	2.423−03
4	2s2p	$^3P^o_2$	0.614 34	0.620 24	0.619 74	0.625 63	8.439+01	8.447+01
5	2s2p	$^1P^o_1$	1.190 97	1.262 89	1.258 72	1.260 08	3.670−10	3.689−10
6	$2p^2$	$^3P_0$	1.599 60	1.626 77	1.626 20	1.637 81	5.290−10	5.290−10
7	$2p^2$	$^3P_1$	1.600 26	1.627 40	1.626 83	1.638 57	5.285−10	5.285−10
8	$2p^2$	$^3P_2$	1.601 40	1.628 45	1.627 88	1.640 09	5.277−10	5.277−10
9	$2p^2$	$^1D_2$	1.721 22	1.789 23	1.785 60	1.799 66	4.304−09	4.315−09
10	$2p^2$	$^1S_0$	2.144 84	2.260 67	2.258 35	2.264 51	2.796−10	2.797−10
11	2s3s	$^3S_1$	3.438 07	3.425 94	3.425 79	3.408 30	1.085−10	1.090−10
12	2s3s	$^1S_0$	3.543 50	3.533 84	3.533 53	3.519 44	3.158−10	3.261−10
13	2s3p	$^1P^o_1$	3.686 28	3.682 49	3.682 04	3.666 19	7.606−11	7.690−11
14	2s3p	$^3P^o_0$	3.699 49	3.689 15	3.689 50	3.673 41	8.132−09	8.135−09
15	2s3p	$^3P^o_1$	3.699 63	3.689 30	3.689 64	3.673 57	7.352−09	7.503−09
16	2s3p	$^3P^o_2$	3.699 95	3.689 61	3.689 95	3.673 87	8.084−09	8.087−09
17	2s3d	$^3D_1$	3.827 74	3.819 16	3.819 40	3.803 01	3.338−11	3.329−11
18	2s3d	$^3D_2$	3.827 77	3.819 19	3.819 43	3.803 08	3.339−11	3.330−11
19	2s3d	$^3D_3$	3.827 85	3.819 27	3.819 51	3.803 18	3.341−11	3.332−11
20	2s3d	$^1D_2$	3.910 79	3.922 87	3.922 53	3.903 10	5.270−11	5.322−11
21	2p3s	$^3P^o_0$	4.240 05	4.237 25	4.237 61	4.223 42	1.350−10	1.361−10
22	2p3s	$^3P^o_1$	4.240 77	4.237 96	4.238 32	4.224 20	1.349−10	1.360−10
23	2p3s	$^3P^o_2$	4.242 28	4.239 44	4.239 79	4.225 77	1.346−10	1.357−10
24	2p3s	$^1P^o_1$	4.310 56	4.328 43	4.326 02	4.313 04	1.116−10	1.129−10
25	2p3p	$^1P_1$	4.382 14	4.379 05	4.379 08	4.363 59	1.111−10	1.149−10
26	2p3p	$^3D_1$	4.415 07	4.417 29	4.417 50	4.400 41	2.567−10	2.605−10
27	2p3p	$^3D_2$	4.415 95	4.418 17	4.418 38	4.401 31	2.567−10	2.605−10
28	2p3p	$^3D_3$	4.417 33	4.419 53	4.419 74	4.402 71	2.564−10	2.602−10
29	2p3p	$^3S_1$	4.443 41	4.441 96	4.441 37	4.425 31	8.947−11	9.104−11
30	2s4s	$^1S_0$		4.498 25	4.498 50	4.483 86	4.572−10	4.845−10
31	2p3p	$^3P_0$	4.503 97	4.504 20	4.504 30	4.493 09	1.836−10	1.834−10
32	2p3p	$^3P_1$	4.504 48	4.504 61	4.504 71	4.493 55	1.831−10	1.828−10
33	2p3p	$^3P_2$	4.505 32	4.505 42	4.505 51	4.494 53	1.830−10	1.827−10
34	2p3d	$^3F^o_2$	4.514 47	4.516 18	4.516 30	4.501 69	1.216−08	1.229−08
35	2p3d	$^3F^o_3$	4.515 17	4.516 85	4.516 97	4.502 45	1.504−08	1.525−08
36	2p3d	$^3F^o_4$	4.516 11	4.517 74	4.517 86	4.503 45	1.539−08	1.561−08
37	2s4s	$^3S_1$	4.538 52	4.529 78	4.529 99	4.511 01	2.991−09	2.960−09
38	2p3d	$^1D^o_2$	4.540 94	4.535 21	4.535 37	4.521 38	7.043−11	7.017−11
39	2p3p	$^1D_2$	4.553 66	4.574 31	4.573 00	4.562 44	1.026−10	1.026−10
40	2s4p	$^3P^o_2$	4.589 87	4.578 88	4.579 08	4.563 36	2.007−10	1.979−10
41	2s4p	$^3P^o_1$	4.589 98	4.578 92	4.579 12	4.563 41	2.032−10	2.004−10
42	2s4p	$^3P^o_0$	4.590 05	4.578 95	4.579 16	4.563 44	2.048−10	2.019−10
43	2p3d	$^3D^o_1$	4.606 95	4.602 49	4.602 86	4.588 18	2.771−11	2.784−11
44	2p3d	$^3D^o_2$	4.607 26	4.602 78	4.603 15	4.588 50	2.771−11	2.784−11
45	2p3d	$^3D^o_3$	4.607 65	4.603 18	4.603 55	4.588 94	2.773−11	2.786−11
46	2s4f	$^1F^o_3$	4.613 61	4.612 81	4.612 77	4.596 52	5.846−11	5.789−11
47	2s4p	$^1P^o_1$	4.620 38	4.621 23	4.620 26	4.603 17	1.402−10	1.497−10
48	2s4d	$^3D_1$	4.660 58	4.648 06	4.648 29	4.632 06	8.657−11	8.679−11
49	2s4d	$^3D_2$	4.660 64	4.648 07	4.648 30	4.632 08	8.660−11	8.683−11
50	2s4d	$^3D_3$	4.660 66	4.648 09	4.648 33	4.632 12	8.666−11	8.688−11
51	2p3d	$^3P^o_2$	4.661 22	4.660 27	4.660 30	4.642 62	6.417−11	6.455−11
52	2p3d	$^3P^o_1$	4.661 68	4.660 80	4.660 82	4.643 12	6.382−11	6.420−11
53	2p3d	$^3P^o_0$	4.661 96	4.661 10	4.661 12	4.643 37	6.365−11	6.403−11
54	2s4d	$^1D_2$	4.689 81	4.687 87	4.687 51	4.668 90	1.214−10	1.275−10
55	2s4f	$^3F^o_2$	4.707 17	4.696 81	4.697 12	4.679 98	2.384−10	2.381−10
56	2s4f	$^3F^o_3$	4.707 25	4.696 91	4.697 22	4.680 10	2.384−10	2.381−10
57	2s4f	$^3F^o_4$	4.707 35	4.697 05	4.697 35	4.680 25	2.385−10	2.382−10
58	2p3p	$^1S_0$		4.740 51	4.732 62	4.720 30	3.556−10	3.648−10
59	2p3d	$^1P^o_1$	4.725 93	4.747 66	4.746 00	4.729 02	4.721−11	4.801−11
60	2p3d	$^1F^o_3$	4.755 56	4.769 96	4.769 41	4.753 16	4.403−11	4.490−11
61	2s5s	$^3S_1$	4.964 71	4.950 00	4.949 63	4.933 29	3.255−10	3.589−10
62	2s5s	$^1S_0$	4.982 18	4.972 88	4.970 94	4.954 49	2.913−10	3.935−10
63	2s5p	$^3P^o_0$		4.997 52	4.997 76	4.981 38	2.076−09	1.739−09
64	2s5p	$^3P^o_1$		4.997 55	4.997 78	4.981 41	2.076−09	1.739−09

Table 1 – *continued*

Index	Configuration	Level	NIST	GRASP1	GRASP2	AS	GRASP1(τ, s)	GRASP2(τ, s)
65	2s5p	$^3P^o_2$		4.997 61	4.997 85	4.981 47	2.086−09	1.745−09
66	2s5p	$^1P^o_1$	5.014 09	5.001 77	5.001 43	4.985 19	1.319−10	2.037−10
67	2s5d	$^3D_1$	5.037 39	5.022 51	5.022 71	5.006 41	1.445−10	1.553−10
68	2s5d	$^3D_2$	5.037 39	5.022 51	5.022 71	5.006 42	1.445−10	1.554−10
69	2s5d	$^3D_3$	5.037 40	5.022 53	5.022 73	5.006 43	1.447−10	1.555−10
70	2s5g	$^3G_3$	5.051 52	5.034 80	5.035 21	5.018 51	9.184−10	9.184−10
71	2s5g	$^3G_4$	5.051 52	5.034 80	5.035 21	5.018 52	9.184−10	9.184−10
72	2s5g	$^3G_5$	5.051 52	5.034 81	5.035 22	5.018 53	9.185−10	9.184−10
73	2s5g	$^1G_4$	5.051 51	5.034 81	5.035 22	5.018 53	9.217−10	9.218−10
74	2s5f	$^3F^o_2$	5.053 63	5.038 49	5.038 88	5.021 98	4.438−10	4.382−10
75	2s5f	$^3F^o_3$	5.053 63	5.038 50	5.038 89	5.022 00	4.437−10	4.381−10
76	2s5f	$^3F^o_4$	5.053 63	5.038 51	5.038 90	5.022 01	4.436−10	4.380−10
77	2s5d	$^1D_2$	5.051 16	5.042 57	5.041 99	5.024 09	1.432−10	1.860−10
78	2s5f	$^1F^o_3$	5.057 49	5.044 65	5.045 00	5.028 31	3.371−10	3.840−10
79	2s6s	$^3S_1$			5.182 33	5.166 04		4.316−10
80	2s6s	$^1S_1$			5.189 64	5.173 27		6.102−10
81	2s6p	$^1P^o_1$			5.204 65	5.188 89		2.043−10
82	2s6p	$^3P^o_0$			5.209 51	5.193 17		2.577−09
83	2s6p	$^3P^o_1$			5.209 52	5.193 19		2.584−09
84	2s6p	$^3P^o_2$			5.209 57	5.193 23		2.597−09
85	2s6d	$^3D_1$			5.224 49	5.208 11		2.465−10
86	2s6d	$^3D_2$			5.224 49	5.208 11		2.467−10
87	2s6d	$^3D_3$			5.224 50	5.208 12		2.470−10
88	2s6d	$^1D_2$			5.235 48	5.217 92		2.622−10
89	2p4s	$^3P^o_0$	5.266 74	5.259 18	5.259 73	5.245 51	2.369−10	2.464−10
90	2p4s	$^3P^o_1$	5.267 54	5.259 90	5.260 45	5.246 27	2.364−10	2.458−10
91	2p4s	$^3P^o_2$	5.269 04	5.261 43	5.261 97	5.247 86	2.354−10	2.446−10
92	2p4s	$^1P^o_1$	5.292 80	5.300 70	5.297 94	5.282 86	1.785−10	2.141−10
93	2s7s	$^3S_1$			5.316 89	5.300 91		3.439−10
94	2p4p	$^1P_1$			5.320 59	5.307 40		1.667−10
95	2s7s	$^1S_1$	5.327 83	5.320 51	5.320 93	5.304 66	1.449−10	8.087−10
96	2p4p	$^3D_1$	5.337 38	5.331 58	5.331 66	5.317 89	3.046−10	2.702−10
97	2p4p	$^3D_2$	5.338 19	5.332 34	5.332 39	5.318 63	3.061−10	2.680−10
98	2p4p	$^3D_3$			5.333 62	5.319 45		2.625−10
99	2s7p	$^3P^o_0$			5.335 77	5.319 46		3.607−09
100	2s7p	$^3P^o_1$			5.335 78	5.319 87		3.594−09
101	2s7p	$^3P^o_2$	5.339 39	5.333 61	5.335 79	5.319 44	3.061−10	3.566−09
102	2s7d	$^3D_1$			5.346 04	5.329 62		4.400−10
103	2s7d	$^3D_2$			5.346 06	5.329 65		4.484−10
104	2s7d	$^3D_3$			5.346 11	5.329 72		4.649−10
105	2s7p	$^1P^o_1$			5.349 50	5.332 02		1.899−10
106	2s7d	$^1D_2$			5.352 46	5.335 04		2.410−10
107	2p4p	$^3S_1$	5.424 74	5.354 21	5.359 86	5.344 32	1.912−10	3.599−10
108	2p4p	$^3P_0$	5.365 45	5.361 61	5.361 82	5.347 68	2.830−10	2.819−10
109	2p4p	$^3P_1$	5.367 28	5.362 13	5.362 50	5.348 32	2.815−10	2.873−10
110	2p4p	$^3P_2$	3.367 90	5.362 82	5.363 03	5.349 01	2.830−10	2.820−10
111	2p4d	$^1D^o_2$	5.364 53	5.378 15	5.378 29	5.365 13	1.587−10	1.587−10
112	2p4d	$^3F^o_2$		5.380 59	5.380 72	5.367 80	3.877−10	3.808−10
113	2p4d	$^3F^o_3$		5.381 10	5.381 22	5.368 36	4.745−10	4.649−10
114	2p4d	$^3F^o_4$		5.382 17	5.382 29	5.369 49	4.783−10	4.683−10
115	2p4p	$^1D_2$	5.386 14	5.391 46	5.390 79	5.376 24	2.011−10	2.419−10
116	2p4d	$^3D^o_1$	5.410 10	5.402 23	5.402 63	5.387 80	6.071−11	6.232−11
117	2p4d	$^3D^o_2$	5.410 32	5.402 50	5.402 91	5.388 10	6.083−11	6.242−11
118	2p4d	$^3D^o_3$	5.410 85	5.402 96	5.403 36	5.388 58	6.072−11	6.234−11
119	2p4f	$^1F_3$		5.406 97	5.407 38	5.392 87	2.230−10	2.227−10
120	2p4f	$^3F_2$		5.407 84	5.408 25	5.393 85	2.338−10	2.338−10
121	2p4f	$^3F_3$		5.408 06	5.408 47	5.394 07	2.334−10	2.334−10
122	2p4f	$^3F_4$		5.408 28	5.408 69	5.394 31	2.339−10	2.339−10
123	2p4d	$^3P^o_2$		5.414 34	5.416 49	5.401 40	9.892−11	1.028−10
124	2p4d	$^3P^o_1$		5.415 02	5.417 16	5.402 08	9.885−11	1.027−10
125	2p4d	$^3P^o_0$		5.415 37	5.417 51	5.402 42	9.891−11	1.027−10
126	2p4f	$^3G_3$		5.420 33	5.420 74	5.406 07	2.462−10	2.455−10
127	2p4f	$^3G_4$		5.420 95	5.421 36	5.406 72	2.474−10	2.467−10
128	2p4f	$^3G_5$		5.421 99	5.422 41	5.407 80	2.462−10	2.455−10

Table 1 – *continued*

Index	Configuration	Level	NIST	GRASP1	GRASP2	AS	GRASP1(τ, s)	GRASP2(τ, s)
129	2p4f	$^1G_4$		5.426 37	5.426 78	5.412 72	3.091−10	3.099−10
130	2p4f	$^3D_3$		5.429 17	5.429 61	5.415 05	2.434−10	2.442−10
131	2p4f	$^3D_2$		5.429 83	5.430 27	5.415 73	2.434−10	2.442−10
132	2p4f	$^3D_1$		5.430 39	5.430 83	5.416 30	2.433−10	2.441−10
133	2p4f	$^1D_2$		5.435 17	5.435 56	5.421 33	2.516−10	2.513−10
134	2p4d	$^1F^o_3$		5.453 35	5.451 89	5.434 79	4.783−11	5.240−11
135	2p4d	$^1P^o_1$		5.461 39	5.460 63	5.443 10	7.699−11	8.395−11
136	2p4p	$^1S_0$		5.465 30	5.466 81	5.451 06	4.884−10	3.385−10
137	2p5s	$^3P^o_0$		5.698 97	5.699 39	5.685 15	3.312−10	3.770−10
138	2p5s	$^3P^o_1$		5.699 65	5.700 08	5.685 87	3.289−10	3.751−10
139	2p5s	$^3P^o_2$		5.701 24	5.701 66	5.687 52	3.278−10	3.730−10
140	2p5s	$^1P^o_1$		5.715 78	5.717 50	5.702 64	1.773−10	2.597−10
141	2p5p	$^1P_1$		5.731 27	5.731 27	5.717 73	1.250−10	2.131−10
142	2p5p	$^3D_1$		5.735 33	5.735 73	5.721 88	3.233−10	4.209−10
143	2p5p	$^3D_2$		5.735 96	5.736 37	5.722 53	3.416−10	4.324−10
144	2p5p	$^3D_3$		5.737 22	5.737 63	5.723 83	3.415−10	4.323−10
145	2p5p	$^3S_1$		5.745 31	5.746 52	5.732 00	1.563−10	2.709−10
146	2p5p	$^3P_0$		5.749 49	5.749 67	5.735 35	4.219−10	4.432−10
147	2p5p	$^3P_1$		5.750 09	5.750 31	5.736 03	3.995−10	4.283−10
148	2p5p	$^3P_2$		5.750 70	5.750 88	5.736 65	4.213−10	4.428−10
149	2p5d	$^3F^o_2$		5.758 60	5.758 68	5.746 82	3.674−10	3.707−10
150	2p5d	$^3F^o_3$		5.760 08	5.760 18	5.745 20	6.898−10	6.287−10
151	2p5d	$^1D^o_2$		5.760 06	5.760 14	5.746 72	3.714−10	3.817−10
152	2p5d	$^3F^o_4$		5.761 19	5.761 29	5.747 98	7.149−10	6.444−10
153	2p5p	$^1D_2$		5.766 09	5.764 71	5.749 94	2.156−10	3.144−10
154	2p5d	$^3D^o_1$		5.769 98	5.770 38	5.755 82	9.547−11	1.118−10
155	2p5d	$^3D^o_2$		5.770 24	5.770 65	5.756 10	9.649−11	1.128−10
156	2p5d	$^3D^o_3$		5.770 79	5.771 18	5.756 67	9.546−11	1.117−10
157	2p5f	$^1F_3$		5.772 64	5.773 05	5.758 69	4.103−10	4.040−10
158	2p5f	$^3F_2$		5.773 21	5.773 61	5.759 30	4.195−10	4.228−10
159	2p5f	$^3F_3$		5.773 35	5.773 76	5.759 45	4.225−10	4.232−10
160	2p5f	$^3F_4$		5.773 56	5.773 97	5.759 67	4.240−10	4.255−10
161	2p5d	$^3P^o_2$		5.775 14	5.775 69	5.761 14	1.417−10	1.604−10
162	2p5g	$^3G^o_4$		5.775 73	5.776 14	5.762 03	6.497−10	6.498−10
163	2p5g	$^3G^o_3$		5.775 73	5.776 14	5.761 77	6.502−10	6.502−10
164	2p5g	$^1G^o_4$		5.775 94	5.776 35	5.761 79	6.648−10	6.648−10
165	2p5g	$^3G^o_5$		5.775 96	5.776 37	5.761 79	6.652−10	6.652−10
166	2p5d	$^3P^o_1$		5.775 76	5.776 31	5.762 01	1.423−10	1.609−10
167	2p5d	$^3P^o_0$		5.776 08	5.776 62	5.762 08	1.431−10	1.617−10
168	2p5f	$^3G_3$		5.777 65	5.778 06	5.763 58	4.622−10	4.474−10
169	2p5f	$^3G_4$		5.778 17	5.778 58	5.764 12	4.660−10	4.522−10
170	2p5g	$^3H^o_4$		5.779 15	5.779 56	5.765 33	7.815−10	7.815−10
171	2p5g	$^3H^o_5$		5.779 19	5.779 60	5.765 13	7.851−10	7.851−10
172	2p5f	$^3G_5$		5.779 16	5.779 57	5.765 28	4.648−10	4.493−10
173	2p5g	$^3H^o_6$		5.780 48	5.780 89	5.766 66	8.023−10	8.024−10
174	2p5g	$^1H^o_5$		5.780 53	5.780 94	5.766 72	8.072−10	8.072−10
175	2p5g	$^3F^o_4$		5.781 29	5.781 70	5.767 46	6.353−10	6.354−10
176	2p5g	$^1F^o_3$		5.781 32	5.781 73	5.767 49	6.373−10	6.375−10
177	2p5f	$^1G_4$		5.782 18	5.782 59	5.768 37	5.576−10	5.887−10
178	2p5g	$^3F^o_2$		5.782 40	5.782 81	5.768 59	6.339−10	6.339−10
179	2p5g	$^3F^o_3$		5.782 43	5.782 84	5.768 63	6.351−10	6.354−10
180	2p5f	$^3D_3$		5.783 42	5.783 83	5.769 32	3.716−10	3.787−10
181	2p5f	$^3D_2$		5.784 05	5.784 45	5.769 95	3.689−10	3.780−10
182	2p5f	$^3D_1$		5.784 58	5.784 99	5.770 50	3.704−10	3.778−10
183	2p5f	$^1D_2$		5.788 56	5.788 60	5.774 19	2.868−10	3.720−10
184	2p5d	$^1F^o_3$		5.798 46	5.795 64	5.779 26	5.611−11	8.571−11
185	2p5d	$^1P^o_1$		5.804 16	5.800 33	5.783 61	7.734−11	1.145−10
186	2p5p	$^1S_0$		5.817 06	5.802 60	5.786 74	5.982−10	6.616−10
187	2p6s	$^3P^o_0$			5.928 82	5.914 56		5.114−10
188	2p6s	$^3P^o_1$			5.929 46	5.915 21		5.041−10
189	2p6s	$^3P^o_2$			5.931 11	5.916 93		5.034−10
190	2p6s	$^1P^o_1$			5.938 73	5.924 12		2.994−10
191	2p6p	$^1P_1$			5.947 67	5.933 91		2.298−10
192	2p6p	$^3D_1$			5.949 82	5.935 90		4.643−10

Table 1 – *continued*

Index	Configuration	Level	NIST	GRASP1	GRASP2	AS	GRASP1(τ, s)	GRASP2(τ, s)
193	2p6p	$^3D_2$			5.950 30	5.936 35		5.443−10
194	2p6p	$^3D_3$			5.951 59	5.937 69		5.443−10
195	2p6p	$^3S_1$			5.955 59	5.941 23		2.881−10
196	2p6p	$^3P_0$			5.957 46	5.943 09		6.464−10
197	2p6p	$^3P_1$			5.958 24	5.943 92		5.600−10
198	2p6p	$^3P_2$			5.958 69	5.944 39		6.434−10
199	2p6d	$^3F^o_2$			5.962 63	5.948 91		6.150−10
200	2p6d	$^3F^o_3$			5.963 85	5.950 19		8.778−10
201	2p6d	$^1D_2$			5.964 11	5.950 41		4.560−10
202	2p6d	$^3F^o_4$			5.965 01	5.951 41		9.462−10
203	2p6p	$^1D_2$			5.967 54	5.952 65		3.536−10
204	2p6d	$^3D^o_1$			5.969 36	5.954 91		1.706−10
205	2p6d	$^3D^o_2$			5.969 61	5.955 20		1.764−10
206	2p6d	$^3D^o_3$			5.970 26	5.955 88		1.704−10
207	2p6d	$^3P^o_2$			5.972 44	5.958 01		2.400−10
208	2p6d	$^3P^o_1$			5.972 96	5.958 53		2.453−10
209	2p6d	$^3P^o_0$			5.973 22	5.958 79		2.494−10
210	2p6d	$^1F^o_3$			5.985 13	5.969 14		1.134−10
211	2p6d	$^1P^o_1$			5.988 05	5.971 74		1.709−10
212	2p6p	$^1S_0$			5.991 55	5.975 39		9.635−10
213	2p7s	$^3P^o_0$			6.063 57	6.049 29		5.621−10
214	2p7s	$^3P^o_1$			6.064 13	6.049 86		5.370−10
215	2p7s	$^3P^o_2$			6.065 86	6.051 67		5.487−10
216	2p7s	$^1P^o_1$			6.070 22	6.055 69		2.567−10
217	2p7p	$^1P_1$			6.075 64	6.061 74		1.776−10
218	2p7p	$^3D_1$			6.077 01	6.063 06		2.770−10
219	2p7p	$^3D_2$			6.077 25	6.063 25		5.207−10
220	2p7p	$^3D_3$			6.078 59	6.064 65		5.219−10
221	2p7p	$^3S_1$			6.080 45	6.066 15		2.140−10
222	2p7p	$^3P_0$			6.081 59	6.067 18		7.881−10
223	2p7p	$^3P_1$			6.082 50	6.068 16		4.998−10
224	2p7p	$^3P_2$			6.082 84	6.068 50		7.726−10
225	2p7d	$^3F^o_2$			6.084 68	6.070 84		8.750−10
226	2p7d	$^3F^o_3$			6.085 78	6.071 94		1.109−09
227	2p7d	$^1D_2$			6.086 16	6.072 29		4.966−10
228	2p7d	$^3F^o_4$			6.087 00	6.073 25		1.430−09
229	2p7d	$^3D^o_1$			6.088 99	6.074 59		1.894−10
230	2p7p	$^1D_2$			6.088 98	6.073 91		2.467−10
231	2p7d	$^3D^o_2$			6.089 28	6.074 96		2.082−10
232	2p7d	$^3D^o_3$			6.090 01	6.075 70		1.906−10
233	2p7d	$^3P^o_2$			6.091 31	6.076 93		2.605−10
234	2p7d	$^3P^o_1$			6.091 72	6.077 33		2.739−10
235	2p7d	$^3P^o_0$			6.091 93	6.077 53		2.837−10
236	2p7d	$^1F^o_3$			6.100 65	6.084 57		8.995−11
237	2p7d	$^1P^o_1$			6.103 13	6.086 57		1.317−10
238	2p7d	$^1S_0$			6.112 56	6.094 24		4.948−10

NIST: http://www.nist.gov/pml/data/asd.cfm
GRASP1: Energies from the GRASP code for 166 level calculations.
GRASP2: Energies from the GRASP code for 238 level calculations.
AS: Energies from the AS calculations (Fernández-Menchero et al. 2014) for 238 levels.

absorption oscillator strength (f_{ij}) which gives a general idea about the strength of a transition. However, the two parameters, for all types of transition $i \rightarrow j$, are related by the following expression:

$$f_{ij} = \frac{mc}{8\pi^2 e^2}\lambda_{ji}^2 \frac{\omega_j}{\omega_i} A_{ji} = 1.49 \times 10^{-16} \lambda_{ji}^2 \frac{\omega_j}{\omega_i} A_{ji} \qquad (1)$$

where m and e are the electron mass and charge, respectively, c the velocity of light, λ_{ji} the transition energy/wavelength in Å, and ω_i and ω_j the statistical weights of the lower (i) and upper (j) levels, respectively. Similarly, these two parameters are related to the line strength S (in atomic unit, 1 a.u. = 6.460×10^{-36} cm^2 esu^2) by the following expression for E1 transitions:

$$A_{ji} = \frac{2.0261 \times 10^{18}}{\omega_j \lambda_{ji}^3} S^{\rm E1} \quad \text{and} \quad f_{ij} = \frac{303.75}{\lambda_{ji}\omega_i} S^{\rm E1}. \qquad (2)$$

Similar equations for other types of transition may be found in Aggarwal & Keenan (2012).

As for energy levels, we have also calculated A-values from both the GRASP1 and GRASP2 models. In Table 2 we list our calculated energies/wavelengths (λ, in Å), radiative rates (A_{ji}, in s^{-1}), oscillator strengths (f_{ij}, dimensionless), and line strengths

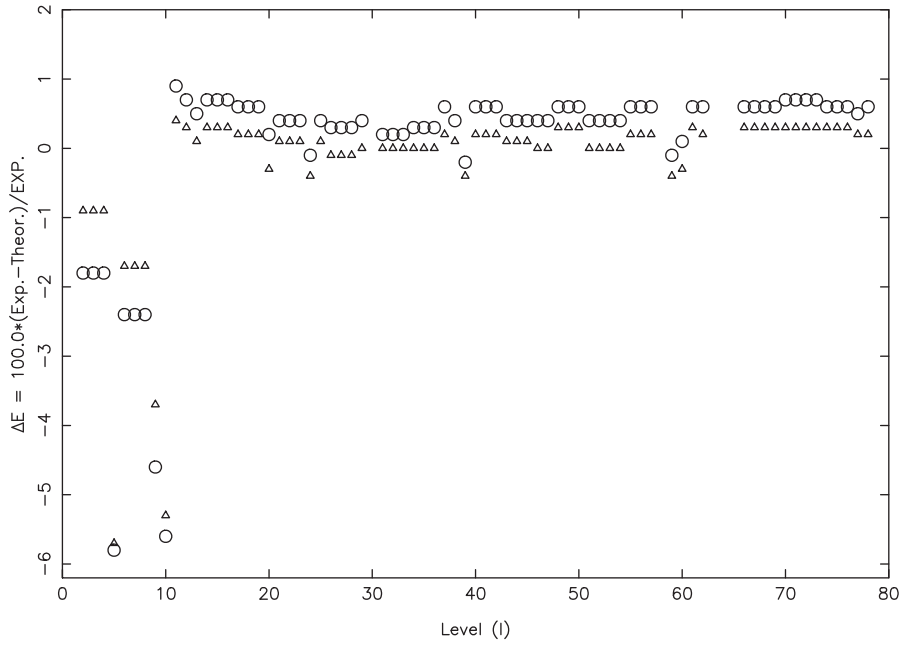

Figure 1. Percentage differences between experimental and theoretical energy levels of N IV. Triangles: present GRASP2 calculations and circles: calculations of Fernández-Menchero et al. (2014) with AS.

Table 2. Transition wavelengths (λ_{ij} in Å), radiative rates (A_{ji} in s^{-1}), oscillator strengths (f_{ij}, dimensionless), and line strengths (S, in atomic units) for electric dipole (E1), and A_{ji} for E2, M1 and M2 transitions in N IV. $a \pm b \equiv a \times 10^{\pm b}$. See Table 1 for level indices. Complete table is available online as Supporting Information.

i	j	λ_{ij}	A_{ji}^{E1}	f_{ij}^{E1}	S^{E1}	A_{ji}^{E2}	A_{ji}^{M1}	A_{ji}^{M2}
1	3	1.473+03	4.128+02	4.030−07	1.955−06	0.000+00	0.000+00	0.000+00
1	4	1.470+03	0.000+00	0.000+00	0.000+00	0.000+00	0.000+00	1.180−02
1	5	7.240+02	2.711+09	6.391−01	1.523+00	0.000+00	0.000+00	0.000+00
1	7	5.602+02	0.000+00	0.000+00	0.000+00	0.000+00	6.996−03	0.000+00
1	8	5.598+02	0.000+00	0.000+00	0.000+00	7.809−02	0.000+00	0.000+00
1	9	5.103+02	0.000+00	0.000+00	0.000+00	3.787+03	0.000+00	0.000+00
...								
...								
...								

(S, in au) for all 8212 E1 transitions among the 238 levels of N IV. These results are in the length form because of their comparatively higher accuracy. The indices used to represent the lower and upper levels of a transition are defined in Table 1. Similarly, there are 10 301 E2, 8136 M1 and 10 353 M2 transitions among the same 238 levels, i.e. the GRASP2 model. Corresponding results from the GRASP1 model among 166 levels can be obtained from the first author (KMA) on request. Additionally, only the A-values are listed in Table 2 for the E2, M1 and M2 transitions, and the corresponding results for f- values can be easily obtained through equation (1).

A general criterion to assess the accuracy of A-values is to look at the ratio (R) of their velocity and length forms. If R is close to unity then the A- (or f-) value is considered to be accurate, although it is only a desirable criterion, not a necessary nor indeed sufficient one. For most (strong) E1 transitions with $f \geq 0.01$, the two forms normally give $R \sim 1$ and their magnitudes do not significantly vary with differing amount of CI (configuration interaction) and/or methods. Among comparatively strong E1 transitions in N IV, for about a third R differs from unity by more than ±20 per cent. For most such transitions R is within a factor of 2, but for a few it has values up to an order of magnitude. Examples of transitions for which R is large are: 5–217 (f = 0.021), 9–81 (f = 0.012) and 20–185 (f = 0.014), i.e. all such transitions are invariably weak. For a few very weak transitions ($f \sim 10^{-5}$ or less) the two forms of f- values differ by up to several orders of magnitude, as also noted for transitions of C III (Aggarwal & Keenan 2015b) and other Be-like ions. Nevertheless, such transitions with very small f-values are unlikely to significantly affect the modelling of plasmas.

Most of the A-values available in the literature for N IV involve levels of the $n \leq 3$ configurations – see for example, Safronova et al. (1999a) and Safronova, Johnson & Derevianko (1999b). However, as for energy levels and collisional data, Fernández-Menchero et al. (2014) have reported results for a larger number of E1 transitions. For most transitions there is satisfactory agreement between the two calculations, but for a few weak(er) ones there are discrepancies of over 50 per cent. Some examples are shown in Table 3, in which results from both the GRASP1 and GRASP2 models are listed. Such discrepancies for weak(er) transitions between any two calculations are quite common (see for example Aggarwal & Keenan 2015b for transitions of C III) and often arise due to the different levels of CI as well as the method adopted – see particularly the weak transitions 2–37, 3–37 and 4–37. Differences in CI may result in cancellation or

Table 3. Comparison of A-values for a few E1 transitions of N IV. $a \pm b \equiv a \times 10^{\pm b}$. See Table 1 for level indices.

I	J	f (GRASP1)	A (GRASP1)	f (GRASP2)	A (GRASP2)	A (AS)	R1	R2
1	43	1.699−05	9.638+05	1.8916−05	1.0730+06	1.930+06	2.0	1.8
2	37	1.753−06	7.183+04	2.3612−08	9.6752+02	2.720+06	37.9	2811.3
3	12	1.401−08	2.868+03	1.2904−08	2.6423+03	1.680+03	1.7	1.6
3	20	2.740−07	1.441+04	2.7037−07	1.4225+04	2.480+04	1.7	1.7
3	30	7.638−05	2.770+07	8.0979−05	2.9377+07	1.430+07	1.9	2.1
3	37	1.425−07	1.750+04	2.3799−06	2.9248+05	4.000+06	228.6	13.7
3	62	3.799−09	1.735+03	4.3647−10	1.9925+02	7.850+02	2.2	3.9
3	77	1.012−07	9.545+03	5.2196−08	4.9224+03	4.370+03	2.2	1.1
4	37	1.489−05	3.048+06	2.5151−05	5.1482+06	1.110+05	27.5	46.4
4	70	1.151−12	1.287−01	9.8121−13	1.0976−01	3.960−01	3.1	3.6
5	6	1.836−07	5.859+02	1.8553−07	6.0372+02	1.010+03	1.7	1.7
5	7	3.061−08	3.267+01	3.1353−08	3.4126+01	5.560+01	1.7	1.6
5	8	2.819−06	1.816+03	2.9598−06	1.9440+03	2.820+03	1.6	1.5
5	11	1.590−07	5.976+03	1.6108−07	6.0762+03	9.430+03	1.6	1.6
5	18	3.059−07	9.634+03	3.1387−07	9.9192+03	2.030+04	2.1	2.0
5	31	1.932−05	4.890+06	1.6592−05	4.2118+06	2.860+06	1.7	1.5
5	48	4.877−08	4.489+03	4.9811−08	4.5969+03	6.980+03	1.6	1.5
5	49	4.652−09	2.569+02	5.2655−09	2.9157+02	1.180+03	4.6	4.0
5	61	3.258−09	3.558+02	3.7610−09	4.1155+02	2.760+03	7.8	6.7
5	67	1.938−08	2.200+03	1.9257−08	2.1914+03	4.250+03	1.9	1.9
5	68	6.116−09	4.166+02	8.6323−09	5.8942+02	2.890+03	6.9	4.9

GRASP1: Present 166 level calculations with the GRASP code.
GRASP2: Present 238 level calculations with the GRASP code.
AS: Calculations of ICFT (Fernández-Menchero et al. 2014) with the AS code.
R1: ratio of GRASP1 and AS A-values, the larger of the two is always in the numerator.
R2: ratio of GRASP2 and AS A-values, the larger of the two is always in the numerator.

Table 4. Comparison of A-values for a few M1 transitions of N IV. $a \pm b \equiv a \times 10^{\pm b}$. See Table 1 for level indices.

I	J	GRASP1	GRASP2	Glass (1983)	Safronova et al. (1999b)
1	7	6.967−3	6.996−3	4.627−3	5.82−3
2	3	3.713−6	3.734−6	4.283−6	4.74−6
2	5	1.255−2	1.249−2	1.315−2	6.36−3
3	4	3.535−5	3.545−5	3.762−5	4.11−5
3	5	1.052−2	1.046−2	3.720−2	5.42−3
4	5	1.637−2	1.630−2	1.629−2	8.42−3
6	7	6.143−6	6.169−6	6.855−6	7.29−6
7	8	2.041−5	2.057−5	2.440−5	2.81−5
7	9	2.325−3	2.286−3	2.055−3	3.33−4
7	10	1.318−1	1.319−1	1.572−1	5.51−2
8	9	7.064−3	6.939−3	6.586−3	1.01−3

GRASP1: Present 166 level calculations with the GRASP code.
GRASP2: Present 238 level calculations with the GRASP code.

addition of different matrix elements and hence affecting the A-(f-) values, particularly for the weak (inter-combination) transitions. However, both the GRASP and AS calculations include the same CI and therefore, the differences noted for transitions in Table 3 are mainly due to the methodology adopted. The A-values for a few M1 transitions are also available in the literature, by Glass (1983) and Safronova et al. (1999b), and in Table 4 we compare our A-values (from GRASP1 and GRASP2) for the transitions in common. As for the weak E1 transitions, for the M1 ones there are also large discrepancies for a few, although the GRASP1 and GRASP2 A-values are very similar. In general, there is a closer agreement between our calculations and those of Glass (1983), and the corresponding results of Safronova et al. (1999b) differ by up to an order of magnitude (see for example the 7–9 transition).

4 LIFETIMES

In contrast to energy levels, there are no direct measurements of radiative rates to compare with theoretical results. However, the A-values are related to the lifetime τ as follows:

$$\tau_j = \frac{1}{\sum_i A_{ji}} \tag{3}$$

and several measurements for levels of N IV are available in the literature. Furthermore, if a single transition dominates the contributions then one can effectively obtain an 'indirect' measurement of the A-value. Therefore, in Table 1 we have also listed our calculated lifetimes, from both the GRASP1 and GRASP2 models. As noted earlier, A-values for E1 transitions are often larger in magnitude and hence dominate the determination of τ. However, we have also included the contributions from E2, M1 and M2 transitions, which can be important for those levels which do not have any dominating E1 connection.

Measurements of τ for levels of N IV (up to 1990) have been compiled by Allard et al. (1990), and are compared in Table 5 with our results from both the GRASP1 and GRASP2 models. Both models yield almost the identical results for all the levels listed in this table, except one, i.e. 2s5p $^1P^o_1$. For this, our GRASP2 value of τ is closer to the measurement. There are several measurements for some levels and therefore we have listed the range of values, with specific results given in table IIIa of Allard et al. (1990). Engström et al. (1981) have also measured τ for the 2s2p $^1P^o_1$ level which was not included by Allard et al. (1990). Their measured value of 0.425 ± 0.015 ns is closer to the lower end of the range (0.44–0.53 ns) listed by Allard et al. (1990), and is only larger than our calculation by 14 per cent (0.37 ns). Similarly, for most of the levels listed in Table 5, there is reasonable agreement (within a few per cent) between theory and measurements. However, there are two exceptions, namely 2p3p ^3P and 2s4s ^3S. For the former, the measured value of 7.83 ± 0.08 ns

Table 5. Comparison of lifetimes (τ, ns) for a few levels of N IV.

Configuration/Level	GRASP1	GRASP2	Allard et al. (1990)
$2s2p\ ^1P^o$	0.367	0.369	0.44–0.53
$2p^2\ ^3P$	0.529	0.529	0.60–0.70
$2p^2\ ^1D$	4.304	4.315	3.10–4.73
$2p^2\ ^1S$	0.280	0.280	0.34
$2s3s\ ^3S$	0.109	0.109	0.13
$2s3s\ ^1S$	0.316	0.326	0.38–0.40
$2s3p\ ^3P^o$	7.845	7.898	7.3–11.5
$2s3d\ ^3D$	0.033	0.033	0.033–0.043
$2s3d\ ^1D$	0.053	0.053	0.050–0.14
$2p3s\ ^3P^o$	0.135	0.136	0.15–0.30
$2p3s\ ^1P^o$	0.112	0.113	0.13–0.30
$2p3p\ ^1P$	0.111	0.115	0.10–0.12
$2p3p\ ^3P$	0.183	0.183	0.18–7.83
$2p3p\ ^1D$	0.103	0.103	0.082–0.11
$2p3p\ ^3D$	0.257	0.261	0.22–0.355
$2p3d\ ^3D^o$	0.027	0.028	0.031–0.23
$2p3d\ ^3P^o$	0.064	0.064	0.078–0.62
$2p3d\ ^1F^o$	0.044	0.045	0.067
$2s4s\ ^3S$	2.991	2.960	0.12
$2s4p\ ^1P^o$	0.140	0.150	0.16–0.55
$2s4p\ ^3P^o$	0.203	0.200	0.17
$2s4d\ ^3D$	0.087	0.087	0.093–0.17
$2s4d\ ^1D$	0.121	0.128	0.12–0.9
$2s4f\ ^3F^o$	0.238	0.238	0.294–0.35
$2s4f\ ^1F^o$	0.058	0.058	0.075
$2s5s\ ^3S$	0.326	0.359	0.37
$2s5p\ ^1P^o$	0.132	0.204	0.32
$2s5f\ ^3F^o$	0.444	0.438	0.43–2.4
$2s5f\ ^1F^o$	0.337	0.384	0.48
$2s5g\ ^3G$	0.918	0.918	0.82–1.22
$2s5g\ ^1G$	0.922	0.922	1.11–1.35

GRASP1: Present 166 level calculations with the GRASP code.
GRASP2: Present 238 level calculations with the GRASP code.

by Desesquelles (1971) is much larger than the 0.18 ± 0.02 ns of Buchet & Buchet-Poulizac (1974) and our result of 0.183 ns, and hence appears to be incorrect. In the case of 2s4s ^{3}S, our calculation of ∼3 ns is larger than the measurement (0.12 ± 0.01 ns) of Buchet & Buchet-Poulizac (1974) by a factor of 25. However, the theoretical results are consistent over a period of time. For example, the dominating contributing E1 transitions are: 2s3p $^3P^o_{0,1,2}$–2s4s $^3S_1$ (i.e. 14/15/16–37) for which our A-values (from both GRASP1 and GRASP2) are 2.8×10^7, 8.8×10^7 and 1.6×10^8 s^{-1}, respectively, whereas those calculated by Tully, Seaton & Berrington (1990) and stored in the NIST data base are 3.01×10^7, 9.02×10^7 and 1.50×10^8 s^{-1}, respectively, i.e. agreeing to better than 10 per cent with our results. Similarly, the A-values of Fernández-Menchero et al. (2014) for the corresponding transitions are 2.9×10^7, 9.4×10^7 and 1.76×10^8 s^{-1}, respectively, again agreeing within 10 per cent with our calculations. Finally, the f-value calculated for the 2s3p $^3P^o$–2s4s ^3S transition by Nussbaumer (1969) is 0.014 whereas our result is 0.016. Therefore, we are confident of our (and other theoretical) results and suspect that the τ measurements for the 2s4s ^3S level, are in error.

Tachiev & Froese Fischer (1999) have calculated A-values for transitions among the lowest 20 levels of Be-like ions, including N IV. They did not report the corresponding τ values, but these are available on their website: http://nlte.nist.gov/MCHF/view.html. Our results are compared with their calculations in Table 6 and there are no discrepancies.

Table 6. Comparison of lifetimes (τ, s) for the lowest 20 levels of N IV. $a \pm b \equiv a \times 10^{\pm b}$.

Index	Configuration	Level	GRASP1	GRASP2	Tachiev & Froese Fischer (1999)
1	$2s^2$	$^1S_0$	.....	.....	.....
2	2s2p	$^3P^o_0$	.....	.....	.....
3	2s2p	$^3P^o_1$	2.471−03	2.423−03	1.726−03
4	2s2p	$^3P^o_2$	8.439+01	8.447+01	8.606+01
5	2s2p	$^1P^o_1$	3.670−10	3.689−10	4.306−10
6	$2p^2$	$^3P_0$	5.290−10	5.290−10	5.606−10
7	$2p^2$	$^3P_1$	5.285−10	5.285−10	5.660−10
8	$2p^2$	$^3P_2$	5.277−10	5.277−10	5.651−10
9	$2p^2$	$^1D_2$	4.304−09	4.315−09	4.266−09
10	$2p^2$	$^1S_0$	2.796−10	2.797−10	3.399−10
11	2s3s	$^3S_1$	1.085−10	1.090−10	1.108−10
12	2s3s	$^1S_0$	3.158−10	3.261−10	3.826−10
13	2s3p	$^3P^o_0$	7.606−11	7.690−11	7.589−11
14	2s3p	$^3P^o_1$	8.132−09	8.135−09	8.339−09
15	2s3p	$^3P^o_2$	7.352−09	7.503−09	8.078−09
16	2s3p	$^1P^o_1$	8.084−09	8.087−09	8.276−09
17	2s3d	$^3D_1$	3.338−11	3.329−11	3.295−11
18	2s3d	$^3D_2$	3.339−11	3.330−11	3.296−11
19	2s3d	$^3D_3$	3.341−11	3.332−11	3.298−11
20	2s3d	$^1D_2$	5.270−11	5.322−11	5.400−11

GRASP1: Energies from the GRASP code for 166 level calculations.
GRASP2: Energies from the GRASP code for 238 level calculations.

5 COLLISION STRENGTHS

The collision strength for electron impact excitation (Ω), a symmetric and dimensionless quantity, is related to the better-known parameter collision cross-section (σ_{ij}), by a simple equation (7) given in Aggarwal & Keenan (2012). As stated in Section 1 (and our work on many Be-like ions), we have adopted the relativistic DARC code (standard and parallelised versions) for the scattering calculations. This code is based on the *jj* coupling scheme and uses the Dirac-Coulomb Hamiltonian in an R-matrix approach. Two sets of calculations have been performed, one (DARC1) with 166 levels of the GRASP1 model, and another (DARC2) with 238 levels of GRASP2. The DARC1 calculations for N IV are larger than those performed for other Be-like ions with $13 \leq Z \leq 32$ (see Aggarwal & Keenan (2015a) and references therein) but are similar to those for C III (Aggarwal & Keenan 2015b). Our DARC2 calculations are even larger, and exactly match in size with those of Fernández-Menchero et al. (2014). For N IV, the adopted R-matrix radius (Ra) and the number of continuum orbitals for each channel angular momentum (NRANG2) are 21.6 au and 55, for DARC1. Correspondingly, the maximum number of channels generated for a partial wave is 828 which leads to the Hamiltonian (H) matrix size of 45 714. For the DARC2 calculations, Ra and NRANG2 are 35.2 au and 88, respectively. The maximum number of channels generated in this calculations is 1116 and the corresponding H-size is 98 478. To achieve convergence of Ω for most transitions and at (almost) all energies, all partial waves with angular momentum $J \leq 40.5$ have been included in both calculations. Furthermore, in both, the contribution of higher neglected partial waves has been included through a top-up procedure, based on the Coulomb-Bethe (Burgess & Sheorey 1974) and geometric series approximations for allowed and forbidden transitions, respectively. Thus care has been taken to ensure the accuracy of our calculated values of Ω, as for other Be-like ions. Finally, values of Ω have been calculated up to energies of 35 and 45 Ryd for DARC1 and DARC2, respectively.

Table 7. Collision strengths for resonance transitions of N IV. $a \pm b \equiv a \times 10^{\pm b}$. See Table 1 for level indices. Complete table is available online as Supporting Information.

Transition		Energy (Ryd)							
i	j	10	15	20	25	30	35	40	45
1	2	1.178−02	6.958−03	4.491−03	3.131−03	2.317−03	1.806−03	1.449−03	1.318−03
1	3	3.535−02	2.089−02	1.349−02	9.412−03	6.968−03	5.438−03	4.369−03	3.975−03
1	4	5.886−02	3.477−02	2.244−02	1.564−02	1.157−02	9.023−03	7.240−03	6.582−03
1	5	6.292+00	7.242+00	7.928+00	8.462+00	8.902+00	9.282+00	9.617+00	9.976+00
1	6	2.418−04	1.257−04	7.227−05	4.522−05	3.020−05	2.110−05	1.583−05	1.238−05
1	7	7.228−04	3.751−04	2.149−04	1.340−04	8.904−05	6.185−05	4.611−05	3.587−05
1	8	1.207−03	6.295−04	3.631−04	2.284−04	1.537−04	1.085−04	8.242−05	6.545−05
1	9	1.423−01	1.372−01	1.344−01	1.328−01	1.319−01	1.313−01	1.311−01	1.320−01
1	10	3.503−02	3.359−02	3.174−02	2.997−02	2.833−02	2.658−02	2.463−02	2.233−02
...									
...									
...									

Subsequently, the values of effective collision strength Υ (see Section 6) are calculated up to $T_e = 1.5 \times 10^6$ K in DARC1, and up to $T_e = 2.0 \times 10^6$ K in DARC2. The temperature of maximum abundance in ionization equilibrium for N IV is only 1.26×10^5 K (Bryans, Landi & Savin 2009), and hence both calculations should cover all plasma applications.

Unfortunately, prior theoretical (or experimental) data for Ω are not available for comparison with our results. At energies above thresholds, Ω varies smoothly and therefore in Table 7 we list our values of Ω for resonance transitions of N IV at energies in the 10–45 Ryd range. These Ω are from our DARC2 calculations and will hopefully be useful for future comparison with experimental and other theoretical results. However, a comparison of Ω made with the DARC1 calculations, for the lowest 78 levels, shows a satisfactory agreement within ∼10 per cent, except for the 1–58 ($2s^2\ ^1S_0 - 2p3p\ ^1S_0$) transition for which the differences are 50 per cent. By contrast, the threshold energy region is often dominated by numerous closed-channel (Feshbach) resonances, as shown in fig. 2 of Fernández-Menchero et al. (2014) for four transitions, namely 1–3 ($2s^2\ ^1S_0 - 2s2p\ ^3P^o_1$), 1–4 ($2s^2\ ^1S_0 - 2s2p\ ^3P^o_2$), 1–5 ($2s^2\ ^1S_0 - 2s2p\ ^1P^o_1$) and 1–9 ($2s^2\ ^1S_0 - 2p^2\ ^1D_2$) for three Be-like ions, C III, Mg IX and Fe XXIII. Similarly, resonances have been shown by us (Aggarwal & Keenan 2012) for six transitions of Ti XIX and two of C III (Aggarwal & Keenan 2015b). Regarding N IV, Ramsbottom et al. (1994) have shown resonances for four transitions, namely $2s^2\ ^1S–2s2p\ ^3P^o$, $2s^2\ ^1S–2p^2\ ^1S$, $2s^2\ ^1S–2s3p\ ^1P^o$ and $2s2p\ ^3P^o–2s2p\ ^1P^o$. We discuss these resonances in the next section.

6 EFFECTIVE COLLISION STRENGTHS

Since Ω does not vary smoothly with energy in the thresholds region, its values are averaged over a suitable distribution of electron velocities to determine the 'effective' collision strength (Υ). For most plasma modelling applications, a Maxwellian distribution of electron velocities is assumed, to obtain Υ from:

$$\Upsilon(T_e) = \int_0^\infty \Omega(E) \exp(-E_j/kT_e)\, \mathrm{d}(E_j/kT_e), \tag{4}$$

where k is Boltzmann constant, T_e the electron temperature in K, and E_j the electron energy with respect to the final (excited) state. Once the value of Υ is known the corresponding results for the excitation $q(i,j)$ and de-excitation $q(j,i)$ rates can be easily obtained from the following equations:

$$q(i,j) = \frac{8.63 \times 10^{-6}}{\omega_i T_e^{1/2}} \Upsilon \exp(-E_{ij}/kT_e) \quad \mathrm{cm^3 s^{-1}} \tag{5}$$

and

$$q(j,i) = \frac{8.63 \times 10^{-6}}{\omega_j T_e^{1/2}} \Upsilon \quad \mathrm{cm^3 s^{-1}}, \tag{6}$$

where ω_i and ω_j are the statistical weights of the initial (i) and final (j) states, respectively, and E_{ij} is the transition energy.

Often, the contribution of resonances over the background collision strengths (Ω_B) is significant (by up to an order of magnitude or even more), but this strongly depends on the type of transition, such as forbidden, semi-forbidden and inter-combination. Similarly, values of Υ are affected by the resonances more at low(er) temperatures than at higher ones. Therefore, it is important to resolve resonances in a fine energy mesh so that their contribution can be properly taken into account. If the energy mesh is too broad then either some of the resonances may be missed (and subsequently Υ may be underestimated) or one may get two consecutive peaks, leading to an overestimation of Υ. On the other hand, if the energy mesh is too fine and the resonances are not too dense, as in the case of C III (Aggarwal & Keenan 2015b), then one may unnecessarily spend time in computational effort without gaining any advantage. Therefore, a careful balance is required in determining the mesh size, and this is important considering the large size of the H matrix.

Since we want to resolve discrepancies between our calculations of Υ and those by Fernández-Menchero et al. (2014), we have performed two full calculations, i.e. DARC1 and DARC2. Our DARC1 calculations are similar to those for C III (Aggarwal & Keenan 2015b), i.e. the energy resolution (ΔE) is generally 0.001 Ryd, although in a few small energy ranges it is 0.002 Ryd. Resonances have been resolved at a total of 3622 energies in the thresholds region. By comparison, our DARC2 calculations are much more extensive because over most of the energy range ΔE is as small as 0.000 045 Ryd. Thus the DARC2 calculations have been performed at over 52 000 energies. Clearly, our DARC1 calculations are (comparatively much) coarser, but have still taken several months to compute. Similarly, the DARC2 calculations have also taken several months in spite of using a parallelised version of the code for this work, as this calculation is much larger, in both the size of the H matrix as well as the energy resolution.

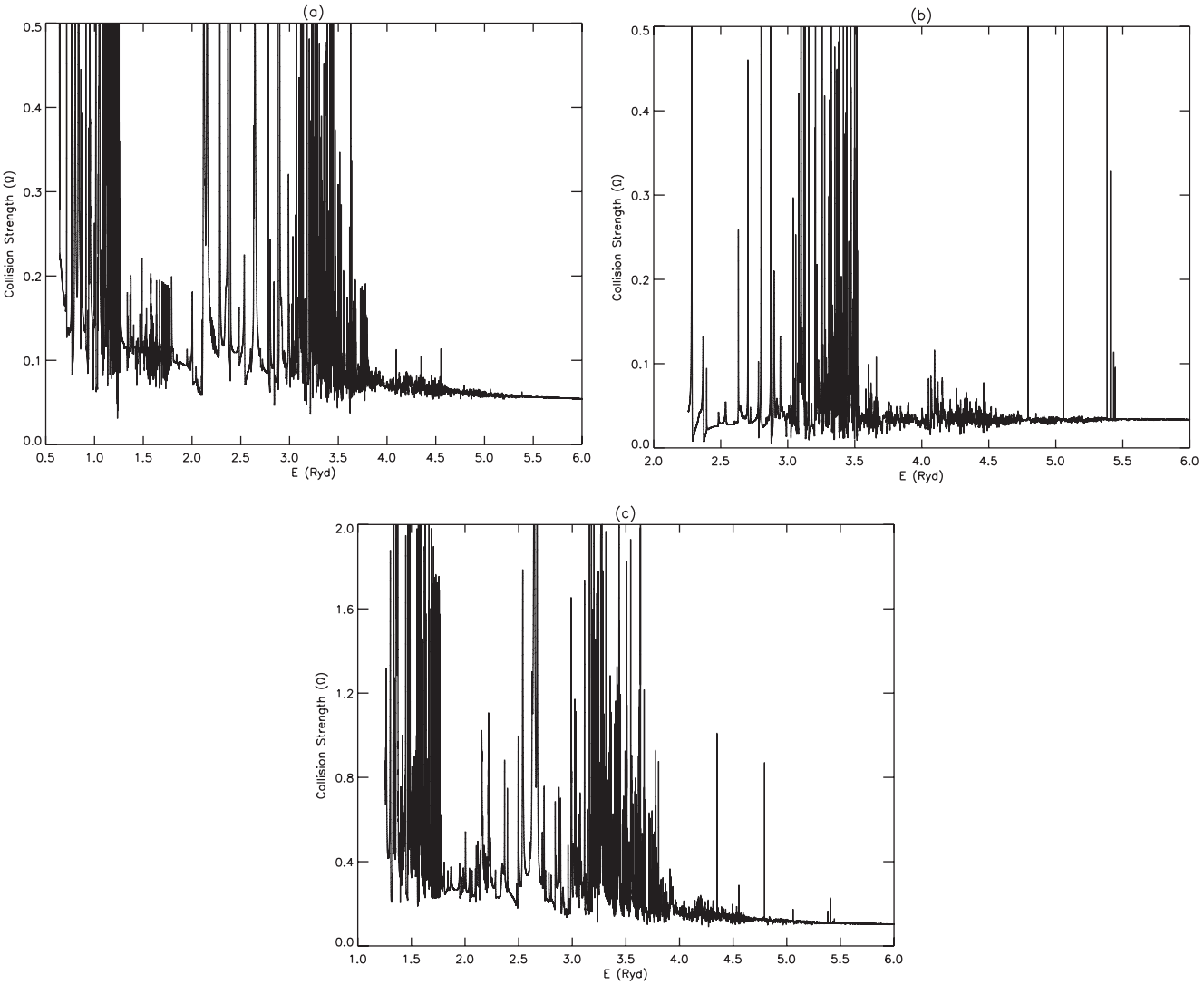

Figure 2. Collision strengths for the (a) 1–3 ($2s^2\ ^1S_0$–$2s2p\ ^3P^o_1$), (b) 1–10 ($2s^2\ ^1S_0$–$2p^2\ ^1S_0$) and (c) 3–5 ($2s2p\ ^3P^o_1$–$2s2p\ ^1P^o_1$) transitions of N IV.

Table 8. Effective collision strengths for transitions in N IV. $a \pm b \equiv a \times 10^{\pm b}$. Complete table is available online as Supporting Information.

Transition		Temperature (log T_e, K)									
i	j	4.50	4.70	4.90	5.10	5.30	5.50	5.70	5.90	6.10	6.30
1	2	1.010−01	8.868−02	7.776−02	6.804−02	5.905−02	5.022−02	4.153−02	3.331−02	2.588−02	1.945−02
1	3	2.969−01	2.620−01	2.307−01	2.025−01	1.761−01	1.500−01	1.242−01	9.967−02	7.748−02	5.826−02
1	4	4.745−01	4.236−01	3.761−01	3.321−01	2.901−01	2.479−01	2.056−01	1.653−01	1.286−01	9.674−02
1	5	3.066+00	3.146+00	3.258+00	3.417+00	3.642+00	3.954+00	4.373+00	4.909+00	5.523+00	6.001+00
1	6	2.157−03	2.081−03	2.089−03	2.105−03	2.011−03	1.777−03	1.459−03	1.131−03	8.381−04	5.996−04
1	7	6.481−03	6.243−03	6.258−03	6.291−03	6.002−03	5.297−03	4.347−03	3.368−03	2.497−03	1.786−03
1	8	1.088−02	1.045−02	1.045−02	1.048−02	9.989−03	8.816−03	7.237−03	5.610−03	4.160−03	2.978−03
1	9	1.842−01	1.887−01	1.931−01	1.949−01	1.918−01	1.846−01	1.753−01	1.659−01	1.568−01	1.460−01
1	10	4.429−02	4.453−02	4.585−02	4.614−02	4.487−02	4.272−02	4.049−02	3.846−02	3.645−02	3.374−02
...											
...											
...											

Before we discuss our results of Υ, in Fig. 2 (a,b and c) we show resonances (from the DARC2 calculations) for three transitions, namely $2s^2\ ^1S_0$–$2s2p\ ^3P^o_1$ (1–3), $2s^2\ ^1S_0$–$2p^2\ ^1S_0$ (1–10) and $2s2p\ ^3P^o_1$–$2s2p\ ^1P^o_1$ (3–5). The first is an inter-combination transition whereas the other two are forbidden. Similar dense resonances have been detected for many more transitions. Our calculated values of Υ (DARC2) are listed in Table 8 over a wide temperature range up to 2×10^6 K, suitable for application to a wide range of astrophysical (and laboratory) plasmas. Data at any intermediate temperature can be easily interpolated, because (unlike Ω) Υ is a slowly

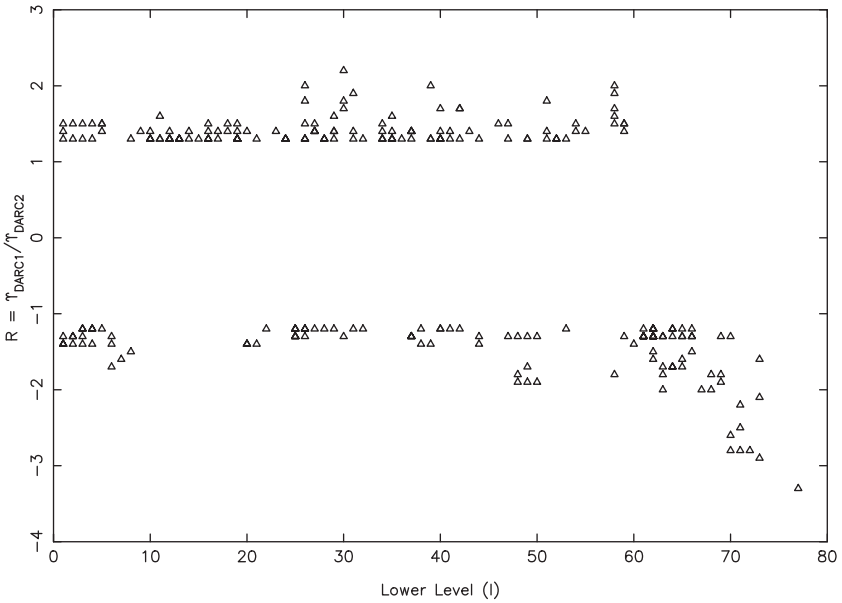

Figure 3. Comparison of DARC1 and DARC2 ϒ for transitions of N IV at $T_e = 1.6 \times 10^5$ K. Negative R values indicate that $\Upsilon_{\rm DARC2} > \Upsilon_{\rm DARC1}$ and only those transitions are shown which differ by over 20 per cent.

varying function of T_e. Our corresponding results from DARC1 are not listed here but can be obtained from the first author (KMA) on request. As noted in Section 1, the most recent and extensive corresponding data available for ϒ are those by Fernández-Menchero et al. (2014). Similar to our work, they have adopted the (semi-relativistic) R-matrix code, resolved resonances in a fine energy mesh (∼0.000 09 Ryd), averaged Ω over a Maxwellian distribution of electron velocities, and reported results for (fine-structure) transitions among 238 levels, over a wide range of electron temperature up to 3.2×10^7 K. However, they divided their calculations into two parts. For $J \leq 11.5$ they performed electron *exchange* calculations but neglected this for higher J values. This should not affect the accuracy of the calculations. However, for higher J their ΔE was coarser (0.009 Ryd), which sometimes may be a limiting source of error in calculating ϒ. By contrast, our calculations have the same energy resolution for all partial waves. Similarly, they calculated values of Ω up to an energy of about 17 Ryd, and beyond that dipole and Born limits were used to extrapolate results up to infinite energy, whereas we have determined Ω up to 35 and 45 Ryd for DARC1 and DARC2, sufficient to calculate ϒ in the temperature range of interest. This is (perhaps) a crucial difference between the two methodologies and hence a major source of discrepancy, as already noted in Aggarwal & Keenan (2015a). To address the discrepancies in ϒ, we now undertake detailed comparisons between different sets of results.

We first compare our values of ϒ from DARC1 and DARC2, to test the conclusion of Fernández-Menchero et al. (2015) that differences in atomic structure (i.e. the size of a calculation) can give rise to the large discrepancies noted by them. We confine this comparison to transitions among the lowest 78 levels, because all calculations have the same ordering for these, as seen in Table 1. We have made these comparisons at three temperatures of: TE1=3.2 $\times 10^3$, TE2=1.6×10^5 and TE3=8.0×10^5 K. TE1 is the lowest temperature at which Fernández-Menchero et al. (2014) have calculated their results and TE2 is closer to the most appropriate value for astrophysical applications (Bryans et al. 2009). At TE1, among the lowest 78 levels (3003 transitions), the ϒ from DARC1 and DARC2 differ by over 20 per cent for 21 per cent of the transitions. For most, $\Upsilon_{\rm DARC2}$ are larger, generally within a factor of 2, but for about 1 per cent of the transitions the discrepancies are up to a factor of 10. These differences are clearly understandable, mainly because (i) this is a very low temperature and hence sensitive to the position and magnitude of resonances, (ii) our ΔE in DARC1 is coarse (0.001 Ryd equivalent to 158 K) and hence not suitable for calculations at such low temperatures, and (iii) our DARC2 calculations include more resonances.

A similar comparison at TE2 shows discrepancies for only 8 per cent of the transitions, mostly within a factor of 2 as shown in Fig. 3. For about half of the transitions, $\Upsilon_{\rm DARC2} > \Upsilon_{\rm DARC1}$, and the reverse is true for the rest. In fact, all those transitions which show (comparatively) larger discrepancies (less than a factor of 4) belong to levels higher than 70, and this is clearly due to the inclusion of resonances from additional levels in DARC2. A similar conclusion applies at TE3, as for only 7 per cent of the transitions are there differences of over 20 per cent, and almost all agree within a factor of 2. Indeed, if the same fine(r) energy resolution had been adopted in DARC1, then the differences between the two sets of ϒ might have been even less. Therefore, our conclusion is clearly different (see Aggarwal & Keenan 2015b and particularly their fig. 3) from those of Fernández-Menchero et al. (2015). A larger calculation certainly improves the accuracy of the calculated ϒ, but for most transitions (and particularly at temperatures of relevance) the discrepancies are generally within ∼20 per cent. We now compare our values of ϒ from DARC2 with the ICFT results of Fernández-Menchero et al. (2014).

In Fig. 4 (a,b and c) we show the ratio $R = \Upsilon_{\rm DARC2}/\Upsilon_{\rm ICFT}$ (negative values plot $\Upsilon_{\rm ICFT}/\Upsilon_{\rm DARC2}$ and indicate $\Upsilon_{\rm ICFT} > \Upsilon_{\rm DARC2}$) for all transitions among the lowest 100 levels of N IV at three temperatures of TE1 = 3.2×10^3, TE2=1.6×10^5 and TE3=1.6×10^6 K. The ratio R is shown as a function of transitions from *lower* levels I. At TE1, values of ϒ for about 22 per cent of the 4950 transitions differ by over 20 per cent, and for a majority of these the $\Upsilon_{\rm ICFT}$ are larger (by up to a factor of 6). For transitions for which $\Upsilon_{\rm DARC2}$ are larger the factor is generally below 3, except for three – see Fig. 4a.

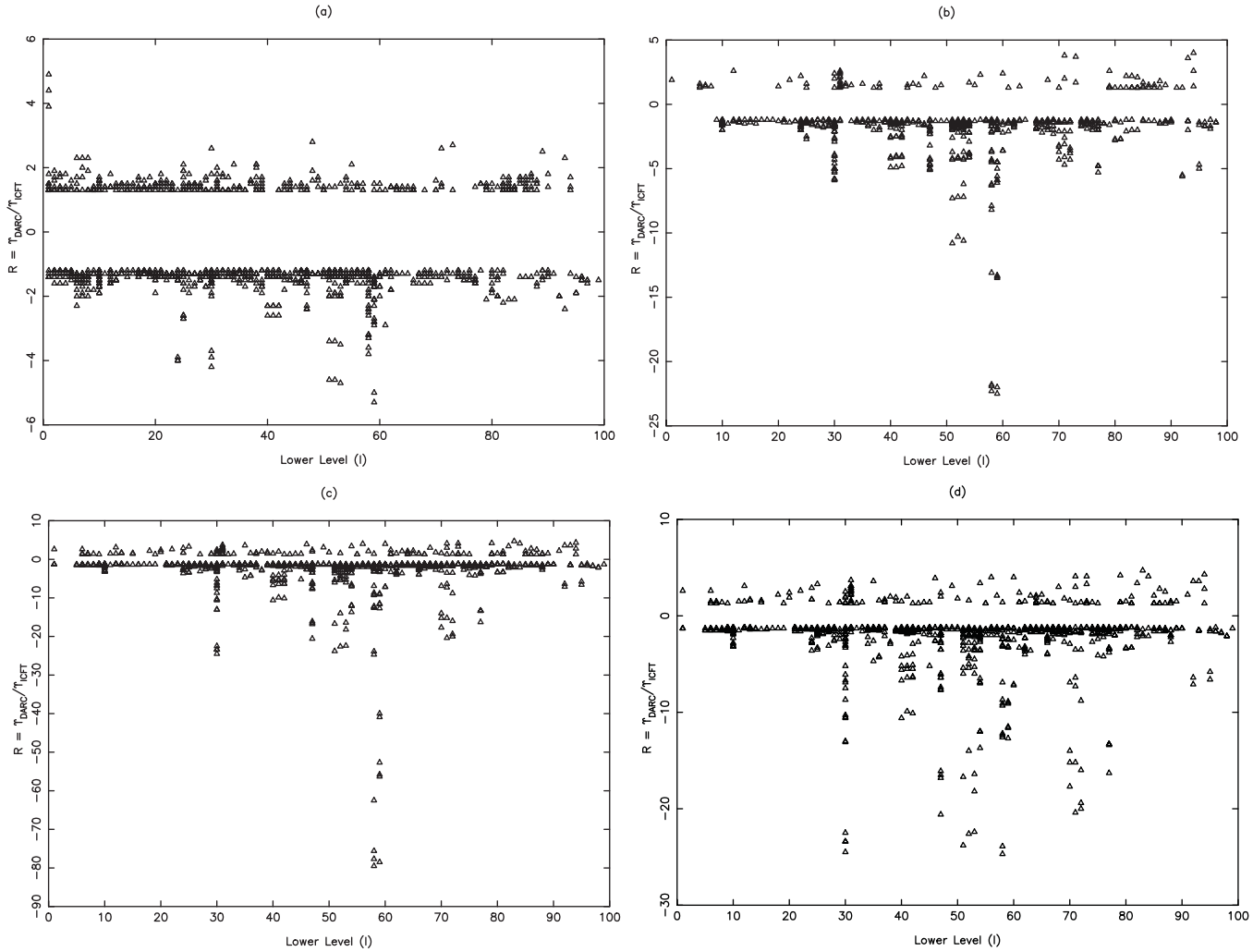

Figure 4. Comparison of DARC2 and ICFT values of ϒ for transitions of N IV at (a) $T_e = 3.2 \times 10^3$ K, (b) $T_e = 1.6 \times 10^5$ K, and (c and d) $T_e = 1.6 \times 10^6$ K. Negative R values plot $\Upsilon_{\rm ICFT}/\Upsilon_{\rm DARC2}$ and indicate that $\Upsilon_{\rm ICFT} > \Upsilon_{\rm DARC2}$. Only those transitions are shown which differ by over 20 per cent.

Considering the fine energy resolution in both calculations and the inclusion of the same number of levels, such discrepancies are not expected. At TE2, a more relevant temperature for plasma modelling applications, the discrepancies are even worse because the $\Upsilon_{\rm ICFT}$ are larger by up to a factor of 25 in most cases – see Fig. 4b. This comparison, although similar to the one shown and discussed earlier (Aggarwal & Keenan 2015a,b) for other Be-like ions, we believe, calls into question the reliability of the calculations by Fernández-Menchero et al. (2014). TE3 corresponds to ∼10 Ryd, and therefore the contribution of resonances should not be as dominant as at lower temperatures (note that the highest threshold considered is at 6.1 Ryd – see Table 1). Therefore, one would expect a (comparatively) better agreement between $\Upsilon_{\rm DARC2}$ and $\Upsilon_{\rm ICFT}$. Unfortunately, the discrepancies become even greater than at lower T_e, as shown in Fig. 4c, because $\Upsilon_{\rm ICFT}$ are larger by up to a factor of 80 in some instances. To obtain a clearer view of the discrepancies we show these again in Fig. 4d, in which the negative vertical scale has been reduced to 30. The ϒ of Fernández-Menchero et al. (2014) appear to be anomalous for many transitions and over a wide range of temperatures. We discuss these further below.

Fernández-Menchero et al. (2015) have argued that instead of the lower levels I in Fig. 4, one should use the *upper* levels J to obtain a better comparison of the two calculations, because in a larger calculation the transitions among the lower levels should not be (much) affected – see their fig. 5b. That should indeed be the case, although it does not apply in the present instance because both calculations are of the same size. Nevertheless, in Fig. 5 (a,b,c and d) we show similar comparisons as those in Fig. 4, but replacing I with J. Only transitions among the lowest ∼50 levels show a reasonably satisfactory agreement, and discrepancies are very large for those belonging to higher levels. This is extremely unsatisfactory, considering that there are 188 levels above the lowest 50. Since both calculations have the same size of atomic structure and use the same R-matrix method a better agreement for transitions among a larger number of levels is expected.

The comparisons of ϒ shown in Figs. 4 and 5 are only for transitions among the lowest 100 levels, as the aim is to provide a clear idea of the discrepancies. Considering all 28 203 transitions among the 238 levels, about 41 per cent, 38 per cent and 44 per cent of these differ by over 20 per cent at TE1, TE2 and TE3, respectively. Furthermore, not only are the values of $\Upsilon_{\rm ICFT}$ larger in a majority of cases, the discrepancies are also greater than shown in Figs 4 and 5, namely up to four orders of magnitude. Examples of such transitions are 59 – 79/85/86 (2p3d $^1P^o_1$ – 2s6s $^3S_1$, 2s6d $^3D_1$, 2s6d

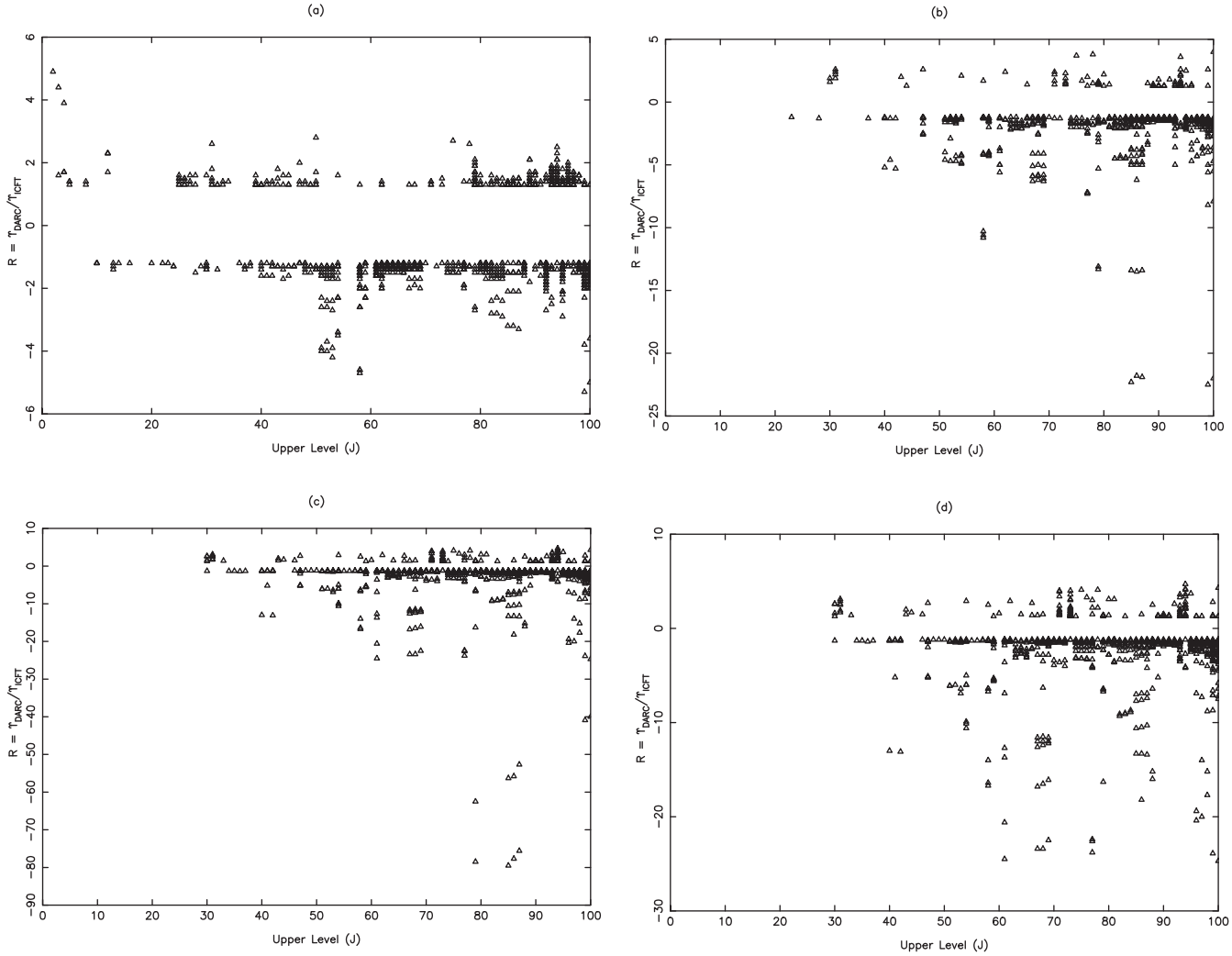

Figure 5. Comparison of DARC2 and ICFT ϒ for transitions of N IV at (a) $T_e = 3.2 \times 10^3$ K, (b) $T_e = 1.6 \times 10^5$ K, and (c and d) $T_e = 1.6 \times 10^6$ K. Negative R values plot $\Upsilon_{\rm ICFT}/\Upsilon_{\rm DARC2}$ and indicate that $\Upsilon_{\rm ICFT} > \Upsilon_{\rm DARC2}$. Only those transitions are shown which differ by over 20 per cent.

$^3D_2$) and there is no ambiguity in the ordering of these levels in our calculations and those of Fernández-Menchero et al. (2014). All of these (and many other) are inter-combination transitions, but the A-values between the two sets of calculations agree within 20 per cent. Furthermore, the f-values for these are $\sim 10^{-6}$ and therefore, such weak transitions should behave as forbidden. Indeed this is the case in our calculations but not in those of Fernández-Menchero et al. (2014). Additionally, since one of the authors (Luis Fernández-Menchero) has kindly provided the Ω data for these transitions, we can confirm that the differences in ϒ values are not due to resonances. Nevertheless, their ϒ at TE3 are 2.4×10^{-1}, 1.4×10^{-1} and 2.3×10^{-1}, respectively, compared to our results of 3.1×10^{-3}, 2.5×10^{-3} and 4.1×10^{-3}, respectively. Similar discrepancies are found towards the lower end of the temperature range, and are partly due to different Ω_B, but mostly due to incorrect trends.

Finally, we discuss just one more example. For the 30–232/233/235 (2s4s $^1S_0$ – 2p7d $^3D^o_3$, $^3P^o_2$, $^3P^o_0$) transitions, the values of $\Upsilon_{\rm ICFT}$ are larger than $\Upsilon_{\rm DARC2}$ by about two orders of magnitude. These transitions are *forbidden* and resonances have (practically) zero contribution. Therefore, both Ω and ϒ should decrease with increasing energy/temperature. This is the case in our work, but not that of Fernández-Menchero et al. (2014). Between $T_e = 3.2 \times 10^3$ and 1.6×10^6 K, the ϒ of Fernández-Menchero et al. (2014) increase from 1.08×10^{-3}, 8.38×10^{-4}, and 1.77×10^{-4} to 9.43×10^{-3}, 1.07×10^{-2} and 2.18×10^{-3}, respectively, whereas our results decrease from 5.24×10^{-4}, 5.83×10^{-4}, and 1.13×10^{-4} to 7.99×10^{-5}, 1.13×10^{-4} and 2.11×10^{-5}, respectively. Unfortunately, for these transitions also neither the Ω_B nor the trends in the ICFT calculations are correct. Therefore, based on the comparisons shown here in Figs 4 and 5, and the above discussion as well as those in Aggarwal & Keenan (2015a,b), we confidently believe that the ϒ results listed by Fernández-Menchero et al. (2014) are indeed overestimated for a large number of transitions and over the entire range of temperatures. The reasons for this could be several as already stated (Aggarwal & Keenan 2015a,b). To recapitulate, these may be: (i) using two different ranges of partial waves with differing amount of ΔE in the thresholds region, (ii) extrapolation of Ω over a very large energy range, and/or (iii) presence of some very large spurious resonances. In particular, we stress that the errors may be in the implementation of the ICFT, not the methodology itself. Indeed this is (in a way) confirmed by the Ω data provided by Luis Fernández-Menchero, because (i) is unlikely to be a major source of error and the authors of the ICFT calculations have checked for (iii), which also does not apply particularly to the

30–232/233/235 transitions. Apart from the high energy behaviour of Ω in the ICFT calculations, their approach (of converting the *LS* results into *LSJ*) unreasonably affects the background values of Ω for some inter-combination transitions.

7 CONCLUSIONS

In this work we have performed two sets of calculations for energy levels, radiative rates, collision strengths, and most importantly effective collision strengths (equivalently electron impact excitation rates) for transitions in Be-like N IV. In the first model, 166 levels of the $n \leq 5$ configurations are considered, whereas the second one is larger with 238 levels, up to $n = 7$. This is mainly to assess the impact of a larger model over that of a smaller one on (particularly) the determination of Υ and to make a direct comparison with the similar calculations of Fernández-Menchero et al. (2014).

For the determination of energy levels and A-values, the GRASP code has been adopted, and (the standard and parallelised versions of) DARC for the scattering calculations. These calculations are similar in methodology to our earlier work on other Be-like ions (Aggarwal & Keenan 2015a,b), but much larger. For the lowest 10 levels, discrepancies in energies with measurements are up to 6 per cent, but agreement is better than 1 per cent for the remaining 228. Additionally, there are no significant discrepancies, in both magnitude or orderings, between our work and that of Fernández-Menchero et al. (2014). The A-values for E1, E2, M1 and M2 transitions have also been reported. For most transitions there are no (major) discrepancies between the two models or with other available data, particularly for a majority of the strong E1 transitions. Lifetimes calculated with these A-values are also found to be in good agreement with other available theoretical and experimental work, and hence (to an extent) confirm the accuracy of our calculations. Based on several comparisons as well as the ratio of the velocity and length forms of the A-values, our listed results are probably accurate to better than 20 per cent for a majority of the strong E1 transitions.

Data have also been reported for collision strengths over a wide range of energy, but only for resonance transitions. However, corresponding results for effective collision strengths are listed for all transitions among the 238 levels of N IV and over a wide range of temperature up to 2.0×10^6 K, well in excess of what should be needed for modelling astrophysical and fusion plasmas. In our smaller model (DARC1) the energy resolution for resonances in thresholds region is comparatively coarser (0.001 Ryd), but is very fine in the larger one, i.e. 0.000 045 Ryd. Nevertheless, for most transitions among the lowest 78 levels, there are no major discrepancies between the two sets of Υ. However, discrepancies with the corresponding results of Fernández-Menchero et al. (2014) are very large (up to four orders of magnitude) for over 40 per cent of the transitions, and over the entire temperature range. These discrepancies are similar to those already found for other Be-like ions (Aggarwal & Keenan 2015a,b), and do not support the conclusion of Fernández-Menchero et al. (2015) that these are due to the size of a calculation. Our assessment is that for a majority of transitions, particularly among most of the lower levels, a larger calculation may improve the accuracy of Υ, but the differences should not be very large. Therefore, the discrepancies found for transitions in many Be-like ions are not due to differences in the size of the atomic structure, but rather the implementation of the method for calculating data. Based on several comparisons shown here and in previous papers, we confidently believe that for most transitions the Υ data of Fernández-Menchero et al. (2014) for Be-like ions are much overestimated. As this is perhaps most likely due to the implementation of ICFT, rather than the code itself, a re-examination of their calculations would therefore be helpful.

ACKNOWLEDGEMENTS

This work has been carried out within the framework of the EURO fusion Consortium and has received funding from the Euratom research and training programme 2014–2018 under grant agreement No. 633053 and from the RCUK Energy Programme (grant number EP/I501045). The views and opinions expressed herein do not necessarily reflect those of the European Commission. We are very thankful to our colleague Dr Connor Ballance for his help in generating data from the DARC2 calculations. We also thank Dr Luis Fernández-Menchero for his kindness in providing Ω data for a few transitions and some clarifications about the ICFT calculations.

REFERENCES

Aggarwal K. M., Keenan F. P., 2012, Phys. Scr., 86, 055301
Aggarwal K. M., Keenan F. P., 2014, MNRAS, 445, 2015
Aggarwal K. M., Keenan F. P., 2015a, MNRAS, 447, 3849
Aggarwal K. M., Keenan F. P., 2015b, MNRAS, 450, 1151
Allard N., Artru M. A., Lanz T., Le Dourneuf M., 1990, A&AS, 84, 563
Badnell N. R., 1997, J. Phys. B, 30, 1
Badnell N. R., Ballance C. P., 2014, ApJ, 785, 99
Berrington K. A., Eissner W. B., Norrington P. H., 1995, Comput. Phys. Commun., 92, 290
Bryans P., Landi E., Savin D. W., 2009, ApJ, 691, 1540
Buchet J. P., Buchet-Poulizac M. C., 1974, J. Opt. Soc. Am., 64, 1011
Burgess A., Sheorey V. B., 1974, J. Phys. B, 7, 2403
Chaplin V. H., Brown M. R., Cohen D. H., Gray T., Cothran C. D., 2009, Phys. Plasmas, 16, 042505
Desesquelles J., 1971, Ann. Phys., 6, 71
Doschek G. A., Feibelman W. A., 1993, ApJS, 87, 331
Dufton P. L., Doyle J. G., Kingston A. E., 1979, A&A, 78, 318
Engström L. et al., 1981, Phys. Scr., 24, 551
Feibelman W. A., Aller A. H., Hyung S., 1992, PASP, 104, 339
Fernández-Menchero L., Del Zanna G., Badnell N. R., 2014, A&A, 566, A104
Fernández-Menchero L., Del Zanna G., Badnell N. R., 2015, MNRAS, 450, 4174
Fosbury R. A. E. et al., 2003, ApJ, 596, 797
Glass R., 1983, Ap&SS, 91, 417
Gu M. F., 2005, At. Data Nucl. Data Tables., 89, 267
Kramida A., Ralchenko Yu, Reader J., NIST ASD Team 2015 NIST Atomic Spectra Database (ver. 5.3), available at http://physics.nist.gov/asd
Machida M., Daltrini A. M., Severo J. H. F., Nascimento I. C., Sanada E. K., Elizondo J. I., Kuznetsov Y. K., 2009, Braz. J. Phys, 39, 270
Nussbaumer H., 1969, MNRAS, 145, 141
Ramsbottom C. A., Berrinhgton K. A., Hibbert A., Bell K. L., 1994, Phys. Scr., 50, 246
Safronova U. I., Derevianko A., Safronova M. S., Johnson W. R., 1999a, J. Phys. B, 32, 3527
Safronova U. I., Johnson W. R., Derevianko A., 1999b, Phys. Scr., 60, 46
Stark D. P. et al., 2014, MNRAS, 445, 3200
Tachiev G., Froese Fischer C., 1999, J. Phys. B, 32, 5805
Tayal S. S., Zatsarinny O., 2015, ApJ, 812, 174
Tully J. A., Seaton M. J., Berrington K. A., 1990, J. Phys. B, 23, 3811
Vanzella E. et al., 2010, A&A, 513, A20

SUPPORTING INFORMATION

Additional Supporting Information may be found in the online version of this article:

Table 2. Transition wavelengths (λ_{ij} in Å), radiative rates (A_{ji} in s^{-1}), oscillator strengths (f_{ij}, dimensionless), and line strengths (S, in atomic units) for electric dipole (E1), and A_{ji} for E2, M1 and M2 transitions in N IV. $a \pm b \equiv a \times 10^{\pm b}$.
Table 7. Collision strengths for resonance transitions of N IV. $a \pm b \equiv a \times 10^{\pm b}$.
Table 8. Effective collision strengths for transitions in N IV. $a \pm b \equiv a \times 10^{\pm b}$.

(http://www.mnras.oxfordjournals.org/lookup/suppl/doi:10.1093/mnras/stw1369/-/DC1).

Please note: Oxford University Press is not responsible for the content or functionality of any supporting materials supplied by the authors. Any queries (other than missing material) should be directed to the corresponding author for the article.

This paper has been typeset from a TEX/LATEX file prepared by the author.